Eur. Phys. J. B **25**, 281–288 (2002)
DOI: 10.1140/epjb/e20020032

THE EUROPEAN PHYSICAL JOURNAL B
EDP Sciences

A study of Peierls instabilities for a two-dimensional t-t′ model

Qingshan Yuan[a]

Experimentalphysik VI, Universität Augsburg, 86135 Augsburg, Germany
and
Pohl Institute of Solid State Physics, Tongji University, Shanghai 200092, PR China

Received 31 July 2001

Abstract. In this paper we study Peierls instabilities for a half-filled two-dimensional tight-binding model with nearest-neighbour hopping t and next nearest-neighbour hopping t' at zero and finite temperatures. Two dimerization patterns corresponding to the same phonon vector (π, π) are considered to be realizations of Peierls states. The effect of imperfect nesting introduced by t' on the Peierls instability, the properties of the dimerized ground state, as well as the competition between two dimerized states for each t' and temperature T, are investigated. It is found: (i). The Peierls instability will be frustrated by t' for each of the dimerized states. The Peierls transition itself, as well as its suppression by t', may be of second- or first-order. (ii). When the two dimerized states are considered jointly, one of them will dominate the other depending on parameters t' and T. Two successive Peierls transitions, that is, the system passing from the uniform state to one dimerized state and then to the other may take place with decrease of temperature. Implications of our results to real materials are discussed.

PACS. 71.45.Lr Charge-density-wave systems – 63.20.Kr Phonon-electron and phonon-phonon interactions

1 Introduction

The Peierls instability, associated with bond-order or charge-density waves, is an important phenomenon in low dimensional materials driven by electron-phonon interaction [1]. The occurance of such an instability is directly relevant to the nesting property of the Fermi surface (FS) in the normal high temperature state of materials. It has been observed in quasi-one dimensional (1D) metals such as polyacetylene $(CH)_x$, blue bronzes $A_{0.3}MoO_3$ (A=K, Rb, Tl) [2], as well as quasi-two dimensional (2D) materials such as purple bronzes AMo_6O_{17} (A=Na, K, Tl) [2–5] and a series of monophosphate tungsten bronzes $(PO_2)_4(WO_3)_{2m}$ with $4 \leq m \leq 14$ [6–9].

Theoretically the description for the Peierls instability was mainly developed for 1D metals, and relatively few investigations are concerned with 2D systems [10–15]. Actually the 2D study of the Peierls instability is not straightforward because of the more complex FS structure as well as richer distortion patterns. For example, in Figure 1 we have shown two possible dimerization patterns for the lattice distortion and the corresponding bond hopping in two dimensions. Both of them correspond to phonons with wave vector (π, π), and their difference is that for pattern (a) the dimerization is in both directions, while it is only in one direction for pattern (b). The simplest model to discuss the Peierls instability in two dimensions is a square lattice tight-binding model with nearest-neighbour (n.n.) hopping t, *i.e.*, the 2D version of the well-known Su-Schrieffer-Heeger (SSH) model [16]. It was originally studied by several authors in connection to high-T_c superconductors [10,11]. At half-filling the FS is perfectly nested with nesting vector $Q = (\pi, \pi)$ so that arbitrarily small electron-lattice coupling [15] will induce a Peierls instability into any one of the dimerized states shown in Figure 1 (if quantum lattice fluctuations are ignored).

The above situation, *i.e.*, perfect nesting of FS is, however, special because it may be easily broken for example, by introduction of next nearest-neighbour (n.n.n.) hopping t'. Actually for real materials, *e.g.*, quasi-2D high-T_c superconductors n.n.n. hopping was found to be important. Also for those quasi-2D materials which show a Peierls instability, perfect nesting of their Fermi surfaces is not satisfied. It is reasonable to adopt a tight-binding model with n.n. and n.n.n. hopping to simulate an essential property of them: the relevance of nesting. Then a question is naturally asked: how is the Peierls instability affected by t'?

It is the purpose of this paper to make a systematical study of Peierls instabilities for a 2D t-t' model, where the nesting property of the FS can be modulated. In contrast, the corresponding problem in the 1D case might be less attractive because the FS is always composed of two points and perfectly nested as long as $t'/t < 0.5$, and then at least in this region t' has no effect on Peierls instability [17]. The 2D problem at zero temperature was

[a] e-mail: qingshan.yuan@physik.uni-augsburg.de

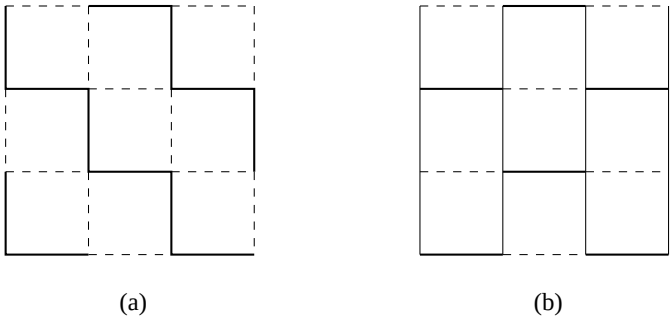

Fig. 1. The lattice distortion patterns (a) and (b). In the figure a thick solid line corresponds to a strong bond with hopping integral $t(1+\delta)$, a dashed line corresponds to a weak bond with hopping integral $t(1-\delta)$, and a thin solid line corresponds to a normal bond with hopping integral t. Both patterns correspond to phonons with wave vector (π,π). The dimerization is along two axes for pattern (a), while only along the x axis for pattern (b).

addressed in an earlier work [15]. It was found that the Peierls instability will be suppressed with increasing t' for each of the two patterns (a) and (b), when they are studied individually. Moreover, when they are considered jointly, one of them was found to dominate the other or reverse when t' is less or greater than some critical value t'_{ab}, *i.e.*, there exists a crossover between the two patterns at $t'=t'_{ab}$. Further one may conjecture that the same behavior should also occur at finite temperatures, and most probably the value t'_{ab} will change with temperature. Then an intriguing phenomenon may arise: at some t', the two dimerized states will dominate successively with change of temperature so that double Peierls transitions (one is between uniform state and dimerized state, the other is between two dimerized states) are expected to take place as a function of temperature. Actually, two successive Peierls transitions were observed in $TlMo_6O_{17}$ [5] and most of the series $(PO_2)_4(WO_3)_{2m}$ [6–9]. So it is interesting to extend the previous work to finite temperatures to discover the above phenomenon. At the same time, new findings at ground state will be supplemented.

Before entering the details we implement a remark on the lattice distortion. Recently, Ono and Hamano studied the 2D Peierls instability numerically in the absence of t' and found that a complex multi-mode distortion pattern has a lower ground state energy than any one of the (π,π) structure presented here [13]. As also described by the authors themselves, however, such a distortion pattern is not unique and may be infinitely degenerate. So it is difficult to extract an explicit pattern for real applications. Moreover, no further confirmation on these new patterns is present at the moment. Thus the question of the real lattice distortion for the 2D Peierls system is still open even in the case of $t'=0$. Under these circumstances we prefer to adopt the two commonly assumed dimerization patterns (a) and (b) as candidates of the Peierls state. These two patterns comply with the nesting vector $Q=(\pi,\pi)$ and realize an unconditional Peierls instability at $t'=0$. Similarly, one may also argue that for each t' and temperature there may exist a lattice distortion structure, though perhaps extremely complicated, with the lowest (free) energy. We have no intention to include all kinds of lattice distortions, which is actually impossible in an analytical treatment on an infinite lattice. Instead, throughout the work we constrain the lattice distortions to the patterns (a) and (b) (although a discussion on a generalization to these two patterns is given in the last section), and based on this, we intend to investigate the presence of t' after fully understanding the $t'=0$ case. This is a natural topic by physical consideration as illustrated in the preceding paragraphs, which is helpful to understand the 2D Peierls instability itself as well as relevant materials even if the assumed dimerized states (a) and (b) might be not the lowest energy Peierls states.

2 Formulation

Our Hamiltonian represents a half filled 2D $t-t'$ model including lattice displacements. It reads [15]:

$$\begin{aligned} H = & -t\sum_{i,j,\sigma}[1+\alpha(u^x_{i,j}-u^x_{i+1,j})](c^\dagger_{i,j,\sigma}c_{i+1,j,\sigma}+\text{h.c.}) \\ & -t\sum_{i,j,\sigma}[1+\alpha(u^y_{i,j}-u^y_{i,j+1})](c^\dagger_{i,j,\sigma}c_{i,j+1,\sigma}+\text{h.c.}) \\ & -t'\sum_{i,j,\sigma}(c^\dagger_{i,j,\sigma}c_{i+1,j+1,\sigma}+c^\dagger_{i,j,\sigma}c_{i+1,j-1,\sigma}+\text{h.c.}) \\ & +\frac{K}{2}\sum_{i,j}[(u^x_{i,j}-u^x_{i+1,j})^2+(u^y_{i,j}-u^y_{i,j+1})^2]\,. \end{aligned} \quad (1)$$

All above notations are conventional: $c^\dagger_{i,j,\sigma}(c_{i,j,\sigma})$ is the creation (annihilation) operator for an electron at site (i,j) with spin σ (i denotes x coordinate and j denotes y coordinate); $u^{x/y}_{i,j}$ is the displacement component of site (i,j) in x/y direction; $t,\ t'$ are n.n and n.n.n. hopping parameters and α is the electron-lattice coupling constant. The last term above describes the lattice elastic potential energy with K the elastic constant. The phonons are treated in adiabatic approximation.

The lattice distortion, as shown in Figure 1, may be explicitly expressed as

$$u^x_{i,j}-u^x_{i+1,j}=(-1)^{i+j}u,\quad u^y_{i,j}-u^y_{i,j+1}=(-1)^{i+j}u$$

for pattern (a) and

$$u^x_{i,j}-u^x_{i+1,j}=(-1)^{i+j}u,\quad u^y_{i,j}-u^y_{i,j+1}=0$$

for pattern (b), where u is the amplitude of dimerization which needs to be determined. Experimentally these two patterns may be differentiated by high resolution X-ray or neutron scattering. For convenience, two dimensionless parameters are defined as follows: the dimerization amplitude $\delta=\alpha u$ and the electron-lattice coupling constant $\eta=\alpha^2 t/K$.

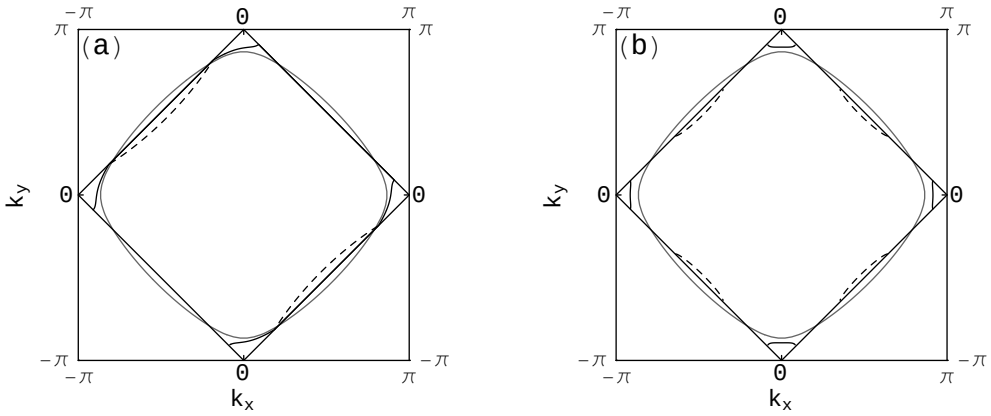

Fig. 2. The Fermi surfaces before dimerization (gray curve) and after dimerization (solid and dashed curves) for $t' = 0.15$ for both patterns. For pattern (a), the FS of the '+' band (dashed curve) is formed just by the two pockets around $(\pi/2, -\pi/2)$ and $(-\pi/2, \pi/2)$; while for pattern (b) it is formed by the four pockets. The '−' band for each case has the large FS (solid curve) with nearly the square shape, except for the cut corners. The square: $|k_x| + |k_y| = \pi$ is the reduced Brillouin zone (also the FS in the case of $t' = \delta = 0$).

The Hamiltonian (1) may be easily diagonalized to give the following electronic spectra in momentum space for patterns (a) and (b), respectively,

$$\begin{aligned}\varepsilon^{\pm}_{\mathbf{k},a} &= -4t' \cos k_x \cos k_y \\ &\quad \pm 2\sqrt{(\cos k_x + \cos k_y)^2 + \delta^2 (\sin k_x + \sin k_y)^2}\ , \\ \varepsilon^{\pm}_{\mathbf{k},b} &= -4t' \cos k_x \cos k_y \\ &\quad \pm 2\sqrt{(\cos k_x + \cos k_y)^2 + \delta^2 \sin^2 k_x}\ . \end{aligned} \tag{2}$$

Before continuing we check the symmetries of the above spectra. It is easy to see that the spectra in both cases are invariant under the same operation: $k_x \to k_x \pm \pi$ and simultaneously $k_y \to k_y \pm \pi$. In addition, the spectra $\varepsilon^{\pm}_{\mathbf{k},a}$ have reflection symmetry: $k_x \to -k_x$ and simultaneously $k_y \to -k_y$, as well as exchange symmetry: $k_x \leftrightarrow k_y$; while the $\varepsilon^{\pm}_{\mathbf{k},b}$ have only the reflection symmetry: $k_x \to -k_x$ *or* $k_y \to -k_y$, or both.

The electronic grand canonical partition function Ξ may be written as:

$$\ln \Xi = 2 \sum_{\mathbf{k},\nu} \ln[1 + \mathrm{e}^{-\beta(\varepsilon^{\nu}_{\mathbf{k}} - \mu)}] \tag{3}$$

with $\beta = 1/k_{\mathrm{B}}T$ (T: temperature) and $\nu = \pm$: band index. The factor 2 in front of the summation includes spin degeneracy. The chemical potential μ is adjusted to yield the right filling, *i.e.*, $N_{\mathrm{e}} = \frac{1}{\beta}\frac{\partial}{\partial \mu} \ln \Xi$. N_{e} is the total electron number, equal to the total number of lattice sites N at half-filling.

The required optimal dimerization parameter δ^* is determined by minimization of the total free energy which is given by

$$F = -\frac{1}{\beta} \ln \Xi + N_{\mathrm{e}} \mu + E_{\mathrm{L}}. \tag{4}$$

Here E_{L} denotes the lattice elastic energy which is, in unit of t, $N\delta^2/\eta$ for pattern (a) and $N\delta^2/(2\eta)$ for pattern (b). Note that E_{L} for (a) is twice of that for (b) under the same δ.

Throughout the paper we take the Bolzmann constant $k_{\mathrm{B}} = 1$ and the n.n. hopping integral t as the energy unit. The parameter η is fixed at a typical value 0.5. The variation of η should not change the results qualitatively, as has been seen at ground state in the earlier work [15]. Also notice that the Hamiltonian with $-t'$ may be mapped onto that with t' at half-filling through the transformation: $c_{i,j,\sigma} \to (-1)^{i+j} c^{\dagger}_{i,j,\sigma}$, so we only consider $t' > 0$ in the following.

3 Results at T = 0

The effects of t' on the Peierls instability were carefully studied at ground state in reference [15], and the main results are summarized here. For each of the two patterns, it was found that t' tends to suppress the Peierls instability. But the details in both cases are different: for (a) the suppression is of first-order while for (b) it is of second-order. The critical values of t' for suppression in both cases are close but slightly different. More interestingly, a crossover between the two dimerized states themselves may take place with change of t'.

After a brief presentation of the above results, our main attention in this section is paid to other useful properties in the ground state, which were not discovered previously. First let us have a look at the variation of the FS before and after dimerization. This helps thoroughly understand the impact of the FS structure on the Peierls instability. We take $t' = 0.15$ for example and plot the Fermi surfaces in Figure 2 for both patterns (also *cf.* the plots of electronic spectra shown later). In this figure, the FS before dimerization is shown by the gray curve in the original Brillouin zone, while after dimerization the Fermi surfaces for the '−' and '+' bands are shown in the reduced Brillouin zone by the solid and dashed curves, respectively. Please note by the way the differences of the

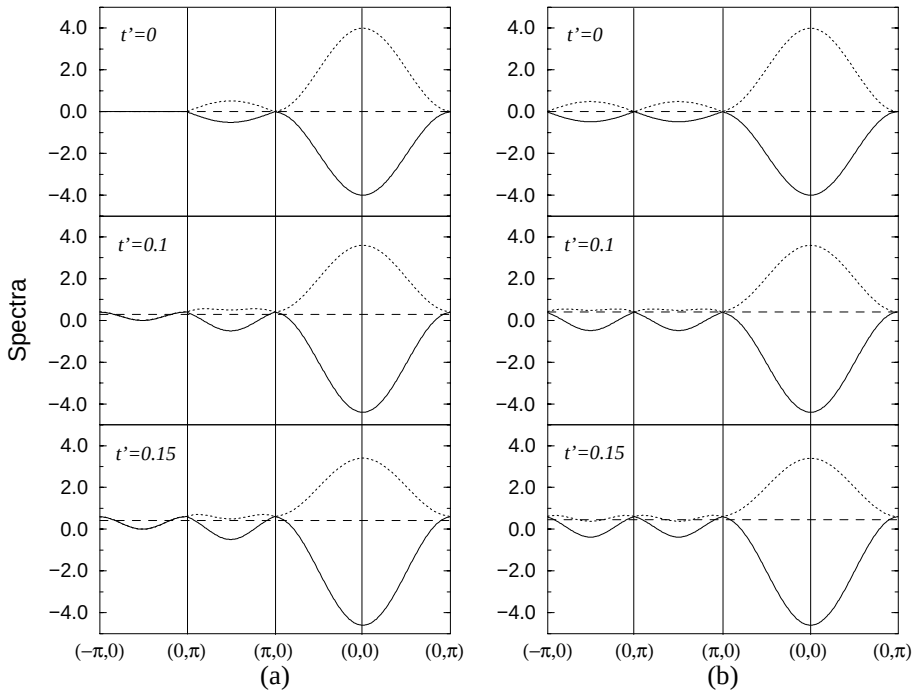

Fig. 3. The electronic spectra in the dimerized states for several t' values for both patterns. The solid and dotted curves in each panel represent energy bands '$-$' and '$+$', respectively, and the dashed horizontal line shows the chemical potential. Note that the two bands in the region $(-\pi, 0)$-$(0, \pi)$ are identical for pattern (a).

FS structures for both patterns which are controlled by the symmetries of the respective spectra addressed above. From Figure 2 a common observation in both patterns is that after dimerization there are a few electrons resting in the '$+$' band, whose energy levels are lifted as seen from equation (2). That is, the energies for this small fraction of electrons are increased by dimerization, leading to a partial cancellation of the energy gain acquired by most of electrons dropping into the '$-$' band. This situation is in contrast to that for $t' = 0$ where the original FS is perfectly nested so that all electrons drop into the '$-$' band with each energy level reduced (at least not raised) by dimerization. Therefore, one may see that the imperfect nesting of the original FS induced by t' is unfavorable to gain the electronic energy *to the largest extend*. And once such a gain is not sufficient to compensate the cost of the elastic energy, the Peierls instability will be prohibited.

Another observation we want to illustrate is that the dimerized state (a) or (b), due to the Peierls transition, is metallic or semi-metallic in two dimensions (even for $t' = 0$) rather than insulating as in one dimension. Actually there is no finite gap opened by the dimerization in any case. To more clearly see this point we have plotted the electronic spectra in the dimerized states for several t' values in Figure 3, as well as their corresponding density of states (DOS), *i.e.*, $\frac{1}{N}\sum_{\mathbf{k},\nu}\delta(\varepsilon - \varepsilon^{\nu}_{\mathbf{k}})$ in Figure 4. The two bands are found to touch or overlap for each t' and for each pattern, as also seen from DOS where no gap appears in each case. We point out that the Peierls instability, when occuring in those real quasi-2D materials, is always associated with a *metal-metal* transition [6].

At this stage, it is worthwhile to mention several points seen from Figure 3: (i) The two bands in the region $(-\pi, 0)$-$(0, \pi)$ are identical for pattern (a). (Thus they are always overlapped.) (ii) The spectra along the path $(-\pi, 0)$-$(0, \pi)$-$(\pi, 0)$ are symmetric about point $(0, \pi)$ for pattern (b), while it is not for pattern (a). This can be also seen from Figure 2. (iii) For pattern (b), the two bands display no overlap for $t' = 0.1$ (in contrast to the case for $t' = 0.15$). Then the ground state energy is simply a summation for the '$-$' band, which becomes t'-irrelevant. So the optimal parameter δ^* should take the same value as that for $t' = 0$, as discussed in the earlier work [15].

At last, we point out that the DOS in each dimerized state for finite t' exhibits the feature of asymmetric double peaks. This could provide characteristic information on some measurable properties like optical absorption in real materials when available.

4 Peierls transitions at T > 0

We discuss finite temperature transitions in this section. For clearness we first look at the results for the two cases of pattern (a) and (b) separately, and then consider the competition between them. The optimal dimerization parameters with change of temperature were calculated for various values of t'. The results for pattern (a) are shown in Figure 5 and those for pattern (b) in Figure 6. A notable common property seen from both figures is that the Peierls transition temperature (denoted as $T_{\rm p}^a$ and $T_{\rm p}^b$ for pattern (a) and (b), respectively) decreases with increase

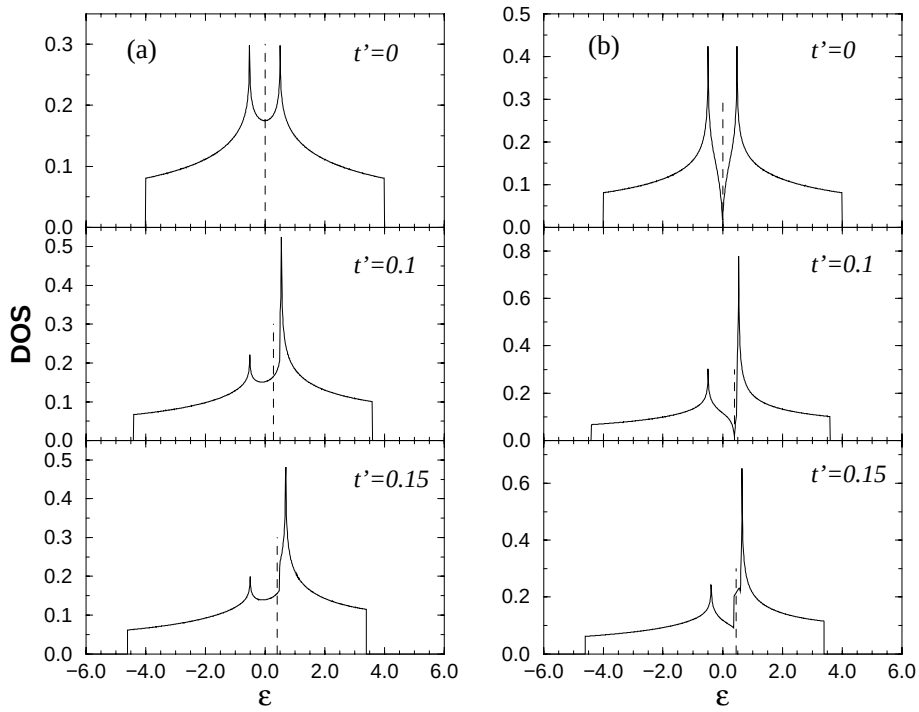

Fig. 4. The density of states (DOS) for each case corresponding to Figure 3. The dashed vertical line in each panel shows the chemical potential.

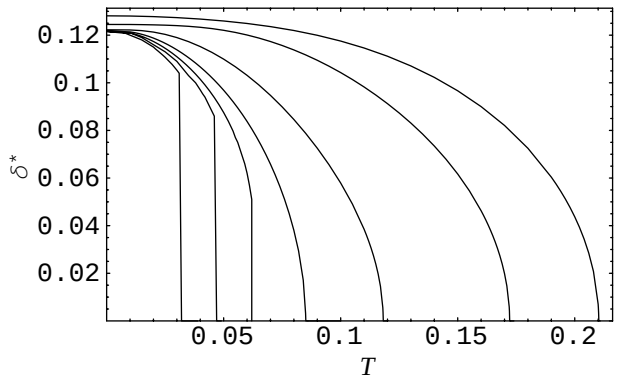

Fig. 5. The optimal dimerization parameter δ^* as a function of temperature T under various values of t' for pattern (a). The curves from right to left correspond to $t' =$ 0, 0.12, 0.16, 0.168, 0.17, 0.171, 0.172, respectively.

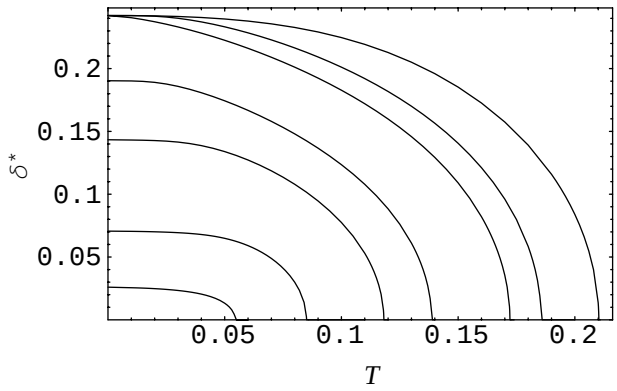

Fig. 6. The same as Figure 5 for pattern (b). The curves from right to left correspond to $t' = 0$, 0.1, 0.12, 0.15, 0.16, 0.168, 0.17, respectively.

of t'. This just means that the n.n.n. hopping t' is unfavorable to the Peierls instability to occur, which is expected and consistent with the results at ground state. It deserves to be pointed out that the lowering of the transition temperature $T_{\rm p}$ with increasing t' is consistent with the experimental findings in the bronzes $(PO_2)_4(WO_3)_{2m}$, where $T_{\rm p}$ was found to increase with m because of better nesting properties [8]. Then we continue to look at the types of transitions in both cases. For pattern (b), the optimal dimerization parameter δ^* goes to zero smoothly with increase of T for each t', *i.e.*, the Peierls transition is always of second-order. However, the type of transition is variant for pattern (a). It is found that for most of t' values the transition is of second-order, while when t' is larger than about 0.17 it becomes of first-order. The explanation for the first-order here is similar to that for the first-order suppression by t' at $T = 0$, which was presented in reference [15].

To see the competition between the two dimerization patterns, one needs to compare the free energies F^* for both patterns at their respective optimal dimerization values for each t' and T. In the following we choose several t' values 0, 0.14, 0.168, 0.17 to show all different kinds of results, see Figures 7–10. In each figure the optimal dimerization parameters and their corresponding free energies (per site) with change of temperature are compared

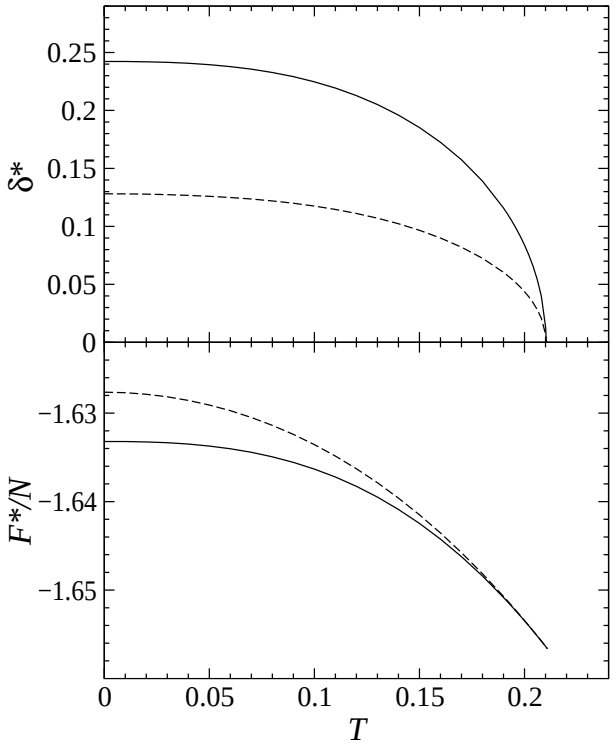

Fig. 7. The optimal values δ^* (upper panel) and the corresponding free energies F^* (lower panel) as a function of T for $t' = 0$. The dashed lines are for pattern (a) and the solid lines are for pattern (b).

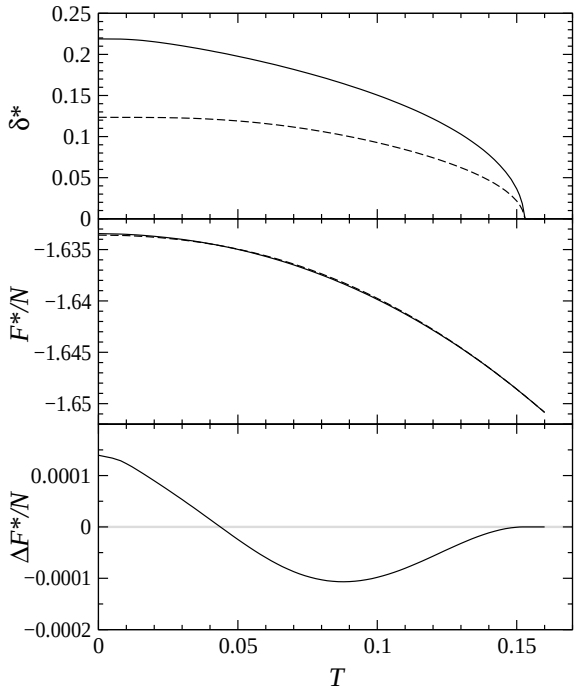

Fig. 8. Similar to Figure 7 but with an additional plot $\Delta F^* = F_b^* - F_a^*$ *vs.* T, for $t' = 0.14$.

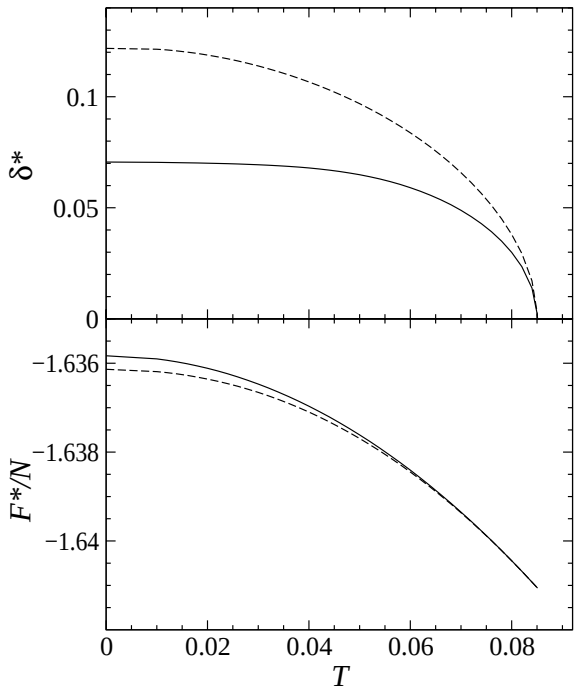

Fig. 9. The same as Figure 7 but for $t' = 0.168$.

for both patterns. We will discuss them in detail in the following.

For the cases of $t' = 0,\ 0.14,\ 0.168$, it is always found that the transition temperatures for both patterns are identical, *i.e.*, $T_{\rm p}^a = T_{\rm p}^b = T_{\rm p}$, but the comparative results on free energies are different. For $t' = 0$ the free energy for pattern (b) F_b^* is always lower than that for pattern (a) F_a^* in the whole temperature region $T < T_{\rm p}$ (see Fig. 7), which means that the dimerized state with pattern (b) is always preferred; while for $t' = 0.168$ the result is exactly the reverse (see Fig. 9). The most interesting case is that for the intermediate $t' = 0.14$, see Figure 8. To more clearly compare the magnitudes of F_a^* and F_b^*, we have plotted their difference $\Delta F^* = F_b^* - F_a^*$ as a function of temperature in the lowest panel, which shows that F_b^* is lower than F_a^* in the intermediate temperature region and then becomes higher for low temperatures. Note that the absolute numerical error for the free energy in our calculations is less than 10^{-8}, so the minor difference ΔF^* is not an artifact. Therefore, in this case the transitions with decreasing temperature may be described as follows: at some critical temperature $T_{\rm c}^1$ the system goes through a Peierls instability into the dimerized state (b). When temperature continues to decrease down to another critical value $T_{\rm c}^2$ the system will turn from the dimerized state (b) into (a). That is to say, in the whole temperature region two successive Peierls transitions take place, as expected in the Introduction.

In addition, for the case of $t' = 0.17$, the transition temperature $T_{\rm p}^a$ becomes different from $T_{\rm p}^b$ and the former is larger, see Figure 10. In addition, the free energy F_a^*

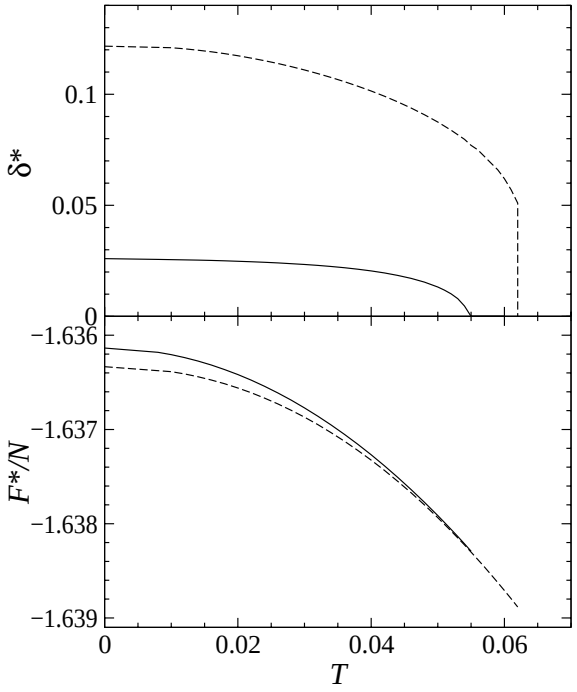

Fig. 10. The same as Figure 7 but for $t' = 0.17$.

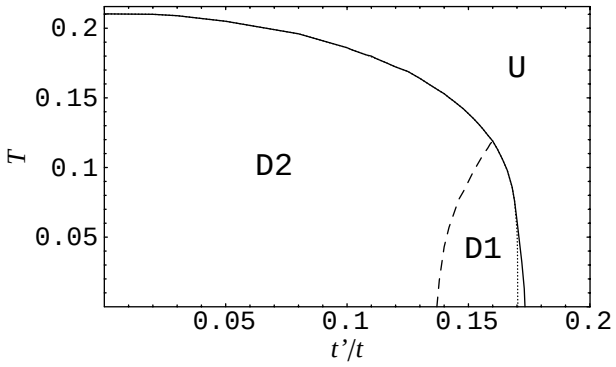

Fig. 11. The phase diagram for different stable states in the parameter space of t' and T. U, D1, D2 represent the uniform state, dimerized state with pattern (a), dimerized state with pattern (b), respectively. The solid and dotted lines are the phase boundaries between U and D1, and D2, respectively, when the two dimerization patterns are considered separately. Note that they are identical for most values of t'. The dashed line differentiates the stable state between D1 and D2. In the narrow area between the solid and dotted line only the D1 state survives.

is always lower than F_b^*. Thus the pattern (a) is always dominant once $T < T_{\rm p}^a$.

With the known results for several typical t' values, we now construct the phase diagram for different stable states in the full parameter space of t' and T. The result is presented in Figure 11, in which most of the above results have been summarized. From Figure 11 the transition temperatures $T_{\rm p}^a$ (solid line) and $T_{\rm p}^b$ (dotted line) with change of t', as well as the competition between two dimerization patterns are clearly seen. Note that the solid and dotted lines are identical for most values of t', and become separate only for a narrow region with large t'. The most exciting result seen from Figure 11 is that the double Peierls transitions, *i.e.*, the system passing the states U→D2→D1 with decrease of temperature, may take place for t' in the region with approximately $0.137 < t' < 0.16$.

5 Discussion and conclusion

In the previous sections, extensive results about the Peierls instability, including the rich phase diagram in the parameter space of t' and T have been discovered. Now we discuss the possible implications of these results to real materials. Although our model may be too simplified when fitting to real quasi-2D Peierls materials, the results obtained are still instructive for the understanding of some experimental findings. (Actually some of instructions have already been presented in the suitable context above.) For real materials, the n.n.n. hopping t' is often indispensable, and moreover, it can be changed by some external conditions, *e.g.*, pressure. Depending on whether the ratio t'/t is enhanced or reduced by the pressure, the Peierls transition temperature is expected to decrease (and even vanish) or increase by it. Experimentally both of possibilities were observed in the real quasi-2D bronzes, see reference [9] and references therein. Our results also suggest that applying pressure (if leading to an enhancement of t'/t) may prevent the materials from the Peierls instability, and then possibly help them enter into the competing superconducting state. Interestingly for the bronze $Li_{0.9}Mo_6O_{17}$, it was found that the superconducting transition temperature is largely increased by pressure, associated with a sharp decrease of the transition temperature of a possible Peierls instability [18]. In particular, our results show two successive Peierls transitions with temperature, a phenomenon which was found in $TlMo_6O_{17}$ [5] and $(PO_2)_4(WO_3)_{2m}$ [6–9]. Essentially, the theoretical and experimental results are similar, *i.e.*, they both originate from the competition between two different lattice distortion patterns. Of course, the real situations are more complicated mainly because of intricate lattice distortions. Nevertheless, our work provides a good example in two dimensions to show double Peierls transitions at finite temperatures. Note that, within the intrinsic limitations (*i.e.*, adiabatic phonons and limited lattice distortion patterns), all results presented here are exact in the thermodynamic limit.

Coming back to the region of Figure 11 where successive transitions U→D2→D1 take place, we further discuss an interesting issue stated as follows. In this figure, it is obvious that the second transition D2→D1 is of first-order. Are there some intermediate states which may smoothly connect D2 and D1? Actually, as a more general dimerization pattern, the lattice distortions may be assumed in the way:

$$u_{i,j}^x - u_{i+1,j}^x = (-1)^{i+j} u_x, \quad u_{i,j}^y - u_{i,j+1}^y = (-1)^{i+j} u_y$$

with a ratio $r = u_y/u_x \in [0, 1]$. The patterns (a) and (b) correspond to the two limiting cases: $r = 1$ and 0,

respectively. If this generalization is included in the calculation, preliminary results give the following scenario with decreasing temperature: first, the transition still happens between the uniform state and the dimerized state (b) (*i.e.*, $r = 0$). This state persists for a range of T and then begins to turn continuously into other dimerized states with $r > 0$. Depending on the value of t', the $r = 1$ state, *i.e.*, the dimerized state (a) may be quickly reached or may not be reached until $T = 0$. Now, the second transition between D1 and other dimerized states becomes of second-order. Detailed results need a more careful calculation.

Finally, we briefly discuss the effects of electron correlations, *e.g.*, the Hubbard on-site U at ground state. For $t' = 0$, it was found that the on-site Coulomb interaction is unfavorable to dimerization in two dimensions as soon as U is present [10,11,20]. This is because the on-site U favors the appearance of antiferromagnetic (AF) order for the 2D half-filled model, while the dimerization tends to stabilize local spin singlets. Thus both, Peierls and AF instabilities, will compete with each other in the presence of finite η and U [20]. On the other hand, the hopping t', which breaks the perfect nesting, will frustrate the Peierls instability as shown here and also the AF instability as shown by several authors [19], when each of them is discussed individually. Then it surely has nontrivial effects on the competition between these two instabilities when they are considered jointly. As far as the Peierls instability is concerned, it is argued that both t' and U may cancel in part their effects when acting simultaneously, although each of them separately tends to suppress it. This topic will be left for future investigation.

In conclusion, the Peierls instabilities for a half-filled 2D t-t' model are thoroughly studied with consideration of two dimerization patterns (a) and (b). The effect of imperfect nesting introduced by t' on the Peierls instability, the properties of the dimerized ground state, as well as the competition between two dimerized states are completely discussed. We have found that the n.n.n. hopping t' will frustrate the Peierls instability for each of the dimerized states when considered separately. Moreover, when the two dimerized states are considered together, they will compete to result in a rich phase diagram in the parameter space of t' and T. Prominently, double Peierls transitions, that is, the system passing from the uniform state to one dimerized state and then to the other may take place with decrease of temperature.

The author would like to thank T. Kopp, T. Nunner, J. Shi, and S.Q. Shen for valuable discussions. This work was financially supported by the Deutsche Forschungsgemeinschaft through SFB 484, the BMBF 13N6918/1, and the National Natural Science Foundation of China.

References

1. G. Grüner, *Density Waves in Solids* (Addison-Wesley, Redwood City, 1994).
2. *Physics and Chemistry of Low-Dimensional Inorganic Conductors*, edited by C. Schlenker, J. Dumas, M. Greenblatt, S. van Smaalen, NATO ASI Series B: Physics Vol. 354 (Plenum, New York, 1996).
3. J. Dumas, C. Schlenker, Int. J. Mod. Phys. B **7**, 4045 (1993).
4. M.H. Whangbo, E. Canadell, P. Foury, J.P. Pouget, Science **252**, 96 (1991).
5. M.L. Tian, S. Yue, J. Shi, S.Y. Li, Y.H. Zhang, J. Phys. Cond. Matt. **13**, 311 (2001); X.K. Qin, J. Shi, H.Y. Gong, M.L. Tian, J.Y. Wei, H. Chen, D.C. Tian, Phys. Rev. B **53**, 15538 (1996); R. Xiong, Q.M. Xiao, J. Shi, H.L. Liu, W.F. Tang, M.L. Tian, D.C. Tian, Mod. Phys. Lett. B **14**, 345 (2000).
6. C. Schlenker, C. Hess, C. Le Touze, J. Dumas, J. Phys. I France **6**, 2061 (1996).
7. E. Wang, M. Greenblatt, I.E. Rachidi, E. Canadell, M.H. Whangbo, S. Vadlamannati, Phys. Rev. B **39**, 12969 (1989); S. Drouard, D. Groult, J. Dumas, R. Buder, C. Schlenker, Eur. Phys. J. B **16**, 593 (2000).
8. J. Dumas, C. Hess, C. Schlenker, G. Bonfait, E. Gomez Marin, D. Groult, J. Marcus, Eur. Phys. J. B **14**, 73 (2000); U. Beierlein, C. Hess, C. Schlenker, J. Dumas, R. Buder, D. Groult, E. Steep, D. Vignolles, G. Bonfait, Eur. Phys. J. B **17**, 215 (2000).
9. J. Beille, U. Beierlein, J. Dumas, C. Schlenker, D. Groult, J. Phys. Cond. Matt. **13**, 1517 (2001).
10. S. Tang, J.E. Hirsch, Phys. Rev. B **37**, 9546 (1988); **39**, 12327 (1989).
11. S. Mazumdar, Phys. Rev. B **36**, 7190 (1987); **39**, 12324 (1989).
12. S. Mazumdar, R.T. Clay, D.K. Campbell, Phys. Rev. B **62**, 13400 (2000).
13. Y. Ono, T. Hamano, J. Phys. Soc. Jpn **69**, 1769 (2000).
14. F. Lin, X.B. Chen, R.T. Fu, X. Sun, Y. Kawazoe, Phys. Stat. Sol. (b) **206**, 559 (1998).
15. Q. Yuan, T. Nunner, T. Kopp, Eur. Phys. J. B **22**, 37 (2001).
16. A.J. Heeger, S. Kivelson, J.R. Schrieffer, W.P. Su, Rev. Mod. Phys. **60**, 781 (1988).
17. Q.S. Yuan (unpublished).
18. C. Escribe-Filippini, J. Beille, M. Boujida, J. Marcus, C. Schlenker, Physica C **162-164**, 427 (1989).
19. See *e.g.*, H.Q. Lin, J.E. Hirsch, Phys. Rev. B **35**, 3359 (1987).
20. Q.S. Yuan, T. Kopp, `cond-mat/0109435`, Phys. Rev. B **65**, 085102 (2002).